ISSN: 0000-0000 www.aristonpubs.com/sciengg-advances https://doi.org/10.69626/sea.2024.0066

RESEARCH ARTICLE

Influence of Strontium Doping on the Electrical Resistivity and Microhardness of Gel Grown Lanthanum Tartrate Crystals

A. Firdous [1], S. Irfan [2], A. H. Pandith [3], I. Nazir [3], N. Ali [2], S. Showket [2], M. Q. Lone[2], G. N. Dar[2]

ABSTRACT: This study investigates the impact of strontium doping on the electrical resistivity and microhardness of gel-grown lanthanum tartrate crystals with stoichiometric compositions of $(La)_{1-x}(Sr)_xC_4H_4O_6.nH_2O$, where x = 0, 0.10, and 0.15. Detailed resistivity measurements reveal a clear trend of decreasing resistivity with increasing strontium concentration. The experimental data conform well to Mott's variable range hopping (VRH) model, indicating that strontium incorporation into the lanthanum tartrate matrix reduces the gap parameters from 190.95 meV to 175.505 meV. This reduction suggests enhanced electrical conductivity, attributed to an increase in carrier density and modified hopping parameters. Specifically, calculations based on the VRH model indicate changes in carrier density, hopping energy, and hopping distances for the polycrystalline spherulitic crystals across all compositions. Additionally, the microhardness of these crystals was evaluated using the Vickers hardness test under varying loads from 0.049 N to 2.9 N. Analysis using Hays and Kendall's law enabled the determination of load-independent Vickers microhardness values for each composition. The results demonstrate that strontium doping not only affects the electrical properties but also enhances the mechanical robustness of lanthanum tartrate crystals, making them more suitable for practical applications requiring both electrical conductivity and mechanical strength. This comprehensive study underscores the potential of strontium-doped lanthanum tartrate crystals in advanced material applications.

Keywords: Lanthanum tartrate, Strontium doping, Electrical resistivity, Microhardness, Mott's variable range hopping

Received: 22 March 2024; Revised: 02 May 2024; Accepted: 12 May 2024; Published Online: 24 May 2024

1. INTRODUCTION

The synthesis and characterization of rare-earth tartrates have garnered significant attention from researchers due to their remarkable structural, electrical, and mechanical properties [1]. The integration of foreign ions into these tartrate matrices has been shown to substantially impact their growth kinetics and alter their physical properties. These modifications can lead to profound changes in the material characteristics, thereby enhancing their potential applications in various fields [2]. The combination of rare-earth elements with tartrate ions results in a complex chemical composition, leading to crystals with unique and potentially valuable properties [3].

In this study, we focus on the growth of pure and strontium-doped lanthanum tartrate (LaT) crystals [4]. The primary objective is to investigate the effects of incorporating alkaline earth elements, specifically strontium, into rare-earth tartrate compositions and to examine the resultant modifications in their mechanical and electrical properties [5]. The growth of pure and strontium-doped LaT was achieved using the silica gel encapsulation technique. This method is well-regarded for producing high-quality crystalline materials [6]. We prepared samples with stoichiometry $(La)_{1-x}(Sr)_xC_4H_4O_6.nH_2O$ (where x = 0, 0.10, 0.15) in polycrystalline spherulitic form and conducted detailed studies on their fundamental characteristics. The comprehensive findings are elaborated in a separate section

[1] Department of Physics, Sri Pratap College, Srinagar-190006, India
[2] Department of Physics, University of Kashmir, Srinagar-190006, India.
[3] Department of Chemistry, University of Kashmir, Srinagar-190006, India

* Author to whom correspondence should be addressed: arfat2phy@gmail.com (A. Firdous)

of this paper.

Our investigation reveals that the spherulitic crystals of pure LaT grown in this study exhibit distinct characteristics compared to those reported in existing literature. Specifically, Kotru et al. reported the growth of LaT crystals with the formula $La_2(C_4H_4O_6)_3.7H_2O$ using the gel method [4]. However, our findings pertain to a different hydration state of LaT, highlighting the diversity in tartrate crystal structures [7-10]. Similar diversity is seen in other tartrate crystals, such as strontium tartrate and gadolinium tartrate, which also exhibit varying waters of hydration [11-15]. Notably, there has been a lack of studies focusing on the microhardness and electrical resistivity of both pure and strontium-doped lanthanum tartrates [16-18]. Prior research on mechanical hardness has predominantly targeted ceramic compositions or single crystals, with no substantial work on the hardness properties of spherulitic crystals [18-22].

The incorporation of strontium into lanthanum tartrate is expected to introduce significant changes in both electrical and mechanical properties. Strontium, being an alkaline earth metal, can alter the electronic environment within the crystal lattice, potentially leading to variations in electrical conductivity and mechanical robustness. Understanding these changes is crucial for developing materials with tailored properties for specific applications.

In this article, we present a comprehensive study on the synthesis, characterization, and evaluation of the electrical resistivity and microhardness of gel-grown pure and strontium-doped lanthanum tartrate (LaT) crystals.

2. EXPERIMENTAL DETAILS

2.1. Preparation of Silica Gel and Crystal Growth

Silica gel was prepared by slowly adding a solution of specified molarity to L-tartaric acid of a given molarity with continuous stirring until the gel set. The gel concentration was maintained at 0.5 M, and the pH of the gel was adjusted to 4. The mixture was allowed to set for a predetermined time, specifically 48 hours. Once the gel had set, lanthanum nitrate solution was carefully added drop by drop along the walls of the tube to avoid breaking the gel. For the growth of strontium-doped LaT crystals, an aqueous solution of strontium nitrate was mixed with the lanthanum nitrate solution before it was introduced to the gel.

The optimized parameters for obtaining better-sized and more numerous spherulites were as follows: the concentration of the upper reactant (lanthanum nitrate solution) was kept at 0.5 M, matching the concentration of L-tartaric acid used in the gel. The growth temperature was maintained within the range of 30-35°C to ensure optimal crystal growth conditions. Additionally, 20 ml of the supernatant liquid was used to facilitate the crystal growth process.

The growth process yielded spherulitic formations throughout the gel, with the well-formed samples selected from the middle of the gel for further analysis. Near the gel-reactant interface, a crust formed due to the instant reaction between the two reactants, resulting in agglomerated tiny spherulites. These spherulitic crystals were powdered in an agate mortar, and the fine powder was pressed into circular pellets with a diameter of 1 cm and a thickness of 0.4 cm using a hydraulic press at a pressure of 10-12 Torr.

2.2. X-Ray Diffraction (XRD) Analysis

The powder XRD patterns of the grown crystals were obtained using a Bruker D-8 Advanced X-Ray diffractometer with Cu Kα radiation (λ=1.5406 Å). The spherulitic formations were carefully examined, and those located in the middle of the tube, whether pure or strontium-doped, were chosen for XRD, electrical, and hardness measurements. The crust near the gel-reactant interface consisted of agglomerated spherulites due to the rapid reaction between the reactants.

2.3. Electrical Resistivity Measurements

The pellets prepared from the powdered spherulitic crystals were mounted on a specially designed four-probe setup for electrical resistivity measurements. These measurements were performed using the standard four-probe technique over a temperature range of 80-300 K, utilizing a closed-cycle refrigerator model CTI-8200. All resistivity measurements were conducted during the warm-up cycle. The four-probe experimental setup was computer-controlled and included a temperature-controlling unit (model LACKE SHORE No.1001D). A Pt/Rh thermocouple was used for temperature measurement, and temperature control was achieved using the LabVIEW program, with a temperature rate set at 1°C/min.

2.4. Microhardness Measurements

Microhardness measurements were carried out on the as-grown surfaces of suitably sized spherulites using an automated Vickers hardness tester (UHL VMHT MOT GERMANY). Reasonably flat portions of the spherulite surface were selected for indentation, with loads ranging from 0.049 N to 2.94 N. In the experimental setup, the indenter approached the target at a velocity of 50 µm/s and impacted the test surface perpendicularly. The diagonal length of each indentation was recorded by computer, and the average of two diagonals for each impression at a particular load was taken for calculation. Measurements were made using a micrometer eyepiece at a magnification of 500:1. The microhardness value (Hv) was calculated using the formula:

$$H_v = 1.8544 \frac{p}{d^2}$$

where P is the applied load in Newtons and d is the diagonal length in micrometers. Error bars were fitted using Origin 6.0 software.

3. RESULTS AND DISCUSSION

3.1. X-ray Diffraction Analysis

The X-ray diffraction (XRD) patterns for pure and strontium-doped lanthanum tartrate (LaT) crystals, with varying compositions, provide critical insights into the structural changes induced by strontium doping. The superimposed powder X-ray diffractogram for the compositions $LaC_4H_4O_6 \cdot 5H_2O$, $La_{0.90}Sr_{0.10}C_4H_4O_6 \cdot 6H_2O$, and $La_{0.85}Sr_{0.15}C_4H_4O_6 \cdot 8H_2O$ are illustrated in Figure 1. These diffractograms reveal distinct variations in the diffraction peaks, which correlate with the strontium content in the crystals. The pure LaT crystal (composition a) exhibits well-defined peaks characteristic of its crystalline structure, indicating a high degree of crystallinity and specific lattice parameters associated with $LaC_4H_4O_6 \cdot 5H_2O$ [23]. With the introduction of strontium into the lattice, as seen in compositions (b) and (c), the diffraction peaks show shifts in position and intensity. These shifts suggest lattice distortion and a change in the unit cell dimensions due to the substitution of La^{3+} ions by the slightly larger Sr^{2+} ions. The change in the number of water molecules associated with the crystal structures is evident. For example, composition (b) with $La_{0.90}Sr_{0.10}C_4H_4O_6 \cdot 6H_2O$ and composition (c) with $La_{0.85}Sr_{0.15}C_4H_4O_6 \cdot 8H_2O$ show differences in their XRD patterns compared to the pure LaT. The additional water molecules likely contribute to variations in the crystal lattice parameters and peak intensities. As strontium concentration increases, notable peak shifts and broadening occur, particularly at higher doping levels (composition c). These changes can be attributed to increased lattice strain and the incorporation of Sr^{2+} ions into the LaT matrix, which affects the overall crystal symmetry and coherence length. The relative intensities of the diffraction peaks vary with strontium content. This can be attributed to differences in the atomic scattering factors of La and Sr, as well as changes in the preferred orientation of the crystallites. The intensity variations also provide information on the degree of crystallinity and the presence of any secondary phases or amorphous content. The absence of additional peaks that do not correspond to the known diffraction patterns of LaT indicates the phase purity of the synthesized crystals. The XRD patterns confirm that the doping process did not introduce significant impurities or secondary phases. By analyzing these diffractograms, we can conclude that strontium doping significantly impacts the structural properties of lanthanum tartrate crystals. The detailed examination of peak positions, intensities, and widths provides valuable information on the crystal lattice modifications, phase transitions, and overall material quality resulting from the incorporation of strontium. These structural insights are crucial for understanding the relationship between the material's composition and its electrical and mechanical properties, as discussed in subsequent sections of this study.

The stoichiometric compositions of these crystals were determined using C-H analysis, EDAX, and FTIR, supplemented by thermo-analytical techniques, the details of which are provided elsewhere. The introduction of foreign ions (Sr) into the LaT lattice resulted in modifications in the patterns, as evidenced by additional peaks detected in the doped LaT. This confirms the presence of the dopant in the parent material. Previous reports by the authors indicate that doping LaT with Sr changes the crystal system from monoclinic (pure lanthanum tartrate) to orthorhombic (Sr-doped lanthanum tartrate). The superimposed XRD traces shown here allow for a direct comparison and highlight the modifications resulting from the introduction of Sr into LaT.

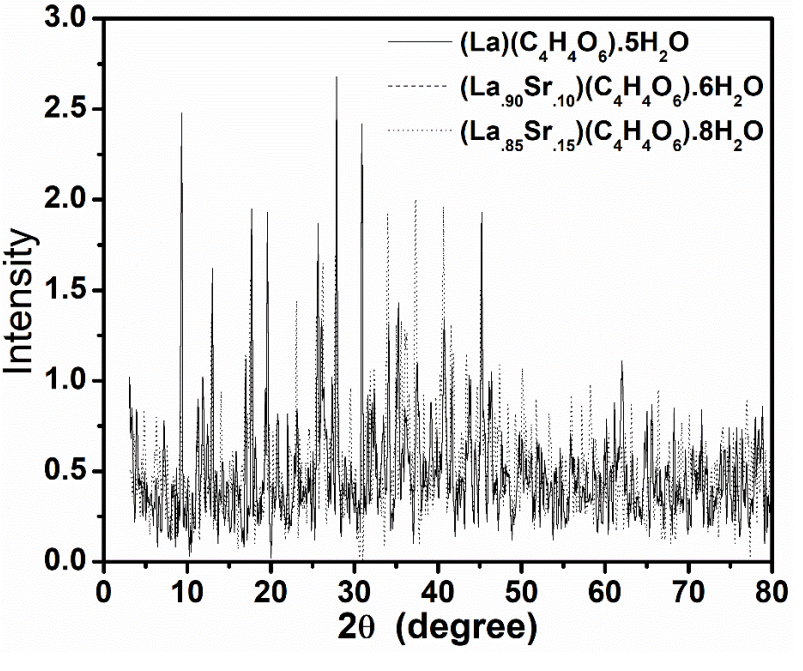

Fig. 1. Powder X-ray diffraction patterns of pure and strontium doped lanthanum tartrate.

3.2. Electrical Resistivity Analysis

The electrical resistivity behavior as a function of temperature for pure and strontium-doped lanthanum tartrate (LaT) crystals with compositions (a) $LaC_4H_4O_6{\cdot}5H_2O$, (b) $La_{0.90}Sr_{0.10}C_4H_4O_6{\cdot}6H_2O$, and (c) $La_{0.55}Sr_{0.15}C_4H_4O_6{\cdot}8H_2O$ is shown in Figure 2. All the samples exhibit semiconducting behavior, characterized by a decrease in resistivity with increasing temperature. The plots clearly demonstrate that the resistivity at room temperature decreases with increasing strontium substitution [24]. Specifically, for 10% strontium doping, the resistivity drops from 28.893 mΩ·cm to 11.252 mΩ·cm at room temperature.

This decrease in resistivity with increasing strontium content is consistent with the well-established phenomenon that the substitution of foreign impurities in polycrystalline materials grown by solid-state reactions leads to carrier doping. This doping decreases the energy gap and consequently reduces the resistivity [25]. Additionally, carrier doping by chemical substitution generally introduces disorder into the system, which can delocalize the carriers at the doping sites. In these localized states, carriers move through a mechanism known as variable-range hopping (VRH).

To understand the effect of disorder-induced localization on the electrical transport properties in this system, the data obtained were fitted using Mott's VRH model. According to Mott's VRH, the expression for electrical resistivity in three dimensions is given by:

$$\rho = \rho_0 \exp(T_0/T)^{1/4} \quad (1)$$

where T_0 is Mott's characteristic temperature, which is related to the density of states at the Fermi level $\{N(E_f)\}$ and the localization length (α) as shown below:

$$T_0 = 18\alpha^3/N(E)k_B \quad (2)$$

The mean hopping distance $R_h(T)$ and hopping energy $E_h(T)$ as functions of temperature are defined by the equations:

$$R_h(T)=(3/8)\,\alpha(T_0/T)^{1/4} \quad (3)$$

$$E_h(T)=[(1/4)(k_B T^{3/4} T_0^{1/4})] \quad (4)$$

To observe the effect of disorder-induced localization on electrical transport, the data were fitted to equation (1), describing Mott's variable-range hopping. The fitted data are plotted as shown in Figure 3. It is interesting to note that the data fit well with the VRH model for temperatures ranging from 258-80 K for $LaC_4H_4O_6{\cdot}5H_2O$, from 265-80 K for $La_{0.90}Sr_{0.10}C_4H_4O_6{\cdot}6H_2O$, and from 273-80 K for $La_{0.85}Sr_{0.15}C_4H_4O_6{\cdot}8H_2O$. The slope of the fitted data yields the energy density at the Fermi level, and T_0 is calculated using equation (2). The calculated value of T_0 is further used in equations (3) and (4) to evaluate the values of R_h and E_h. This indicates that conduction is controlled by disorder-induced localization of charge carriers.

The calculated values summarized in Table 1 demonstrate that both the hopping energy and hopping distance decrease with increasing strontium concentration, indicating a more delocalized carrier state in doped LaT samples. This suggests enhanced electrical conductivity and reduced resistivity due to strontium doping, aligning with the observed experimental data. The electrical resistivity measurements and the fitting to Mott's VRH model reveal that strontium doping introduces significant changes in the electrical transport properties of lanthanum tartrate crystals. The decreased resistivity and modified VRH parameters indicate enhanced carrier mobility and reduced localization effects, which are directly correlated with the increased strontium content. The results underscore the role of disorder-induced localization in enhancing carrier mobility and reducing resistivity, essential for optimizing the performance of material in various electronic applications.

3.3. Microhardness Analysis

Investigating the response of spherulite surfaces to indentation processes provides valuable insights into the mechanical properties of materials, particularly in polycrystalline forms like lanthanum tartrate (LaT). The evaluation of microhardness (Hv) using Mayer's and Hays and Kendall's laws offers a systematic approach to understand how the material's hardness varies with applied load [26].

Mayer's law relates the applied load (P) to the diagonal length (d) of the indentation on the material's surface:

$$P=K_1 d^n \quad (5)$$

where K_1 is a material constant and n is the Mayer's index. When equals 2, it indicates that Hv is independent of the applied load, signifying a crucial mechanical property of the material.

Hays and Kendall's law provides an empirical relationship to determine Hv as a function of load:

$$P\text{-}W = k_2 d^n \quad (6)$$

Here, W represents the Newtonian resistance pressure, and K_2 is another constant. The determination of n involves plotting ln(P-W) against ln d, where the slope and intercept of the resulting graph yield n and K_2. This approach was applied to the spherulitic crystals of both pure and strontium-doped LaT.

Figure 4 illustrates the dependence of Hv on load for pure and strontium-doped lanthanum tartrate compositions, confirming the applicability of Hays and Kendall's law in describing Hv across different loads.

Table 1. Calculations Based on VRH Model.

Samples	ρ (mΩ·cm)	ρ_0 (mΩ·cm)	$N(E_f) \times 10^{19}$ ($eV^{-1}cm^{-3}$)	R_h (Å)	E_h (meV)
$LaC_4H_4O_6 \cdot 5H_2O$	1528.40	15.13	1.42	2.76	190.95
$La_{0.90}Sr_{0.10}C_4H_4O_6 \cdot 6H_2O$	1131.27	8.73	1.66	1.51	184.79
$La_{0.85}Sr_{0.15}C_4H_4O_6 \cdot 8H_2O$	499.60	4.30	2.00	1.43	175.50

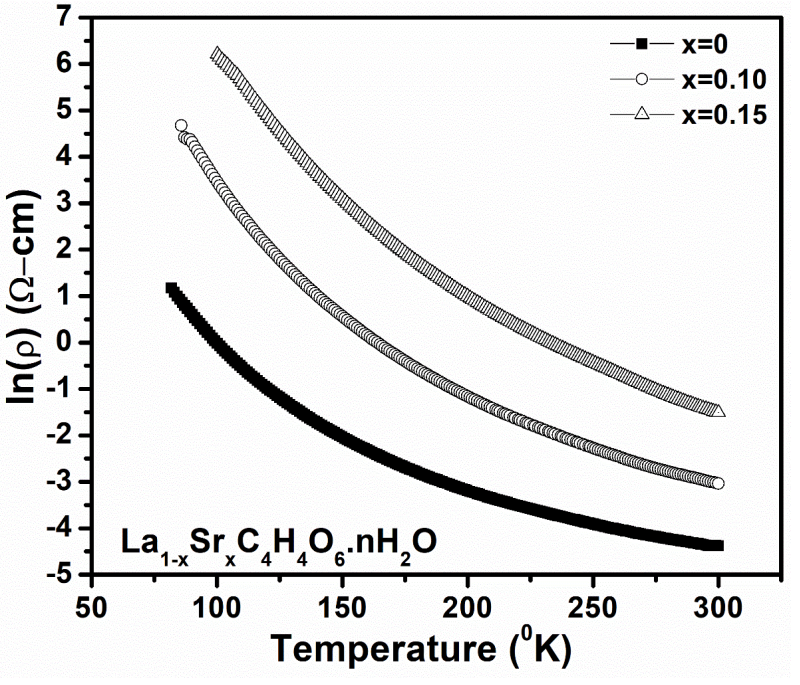

Fig. 2. DC resistivity of pure and doped lanthanum tartrate.

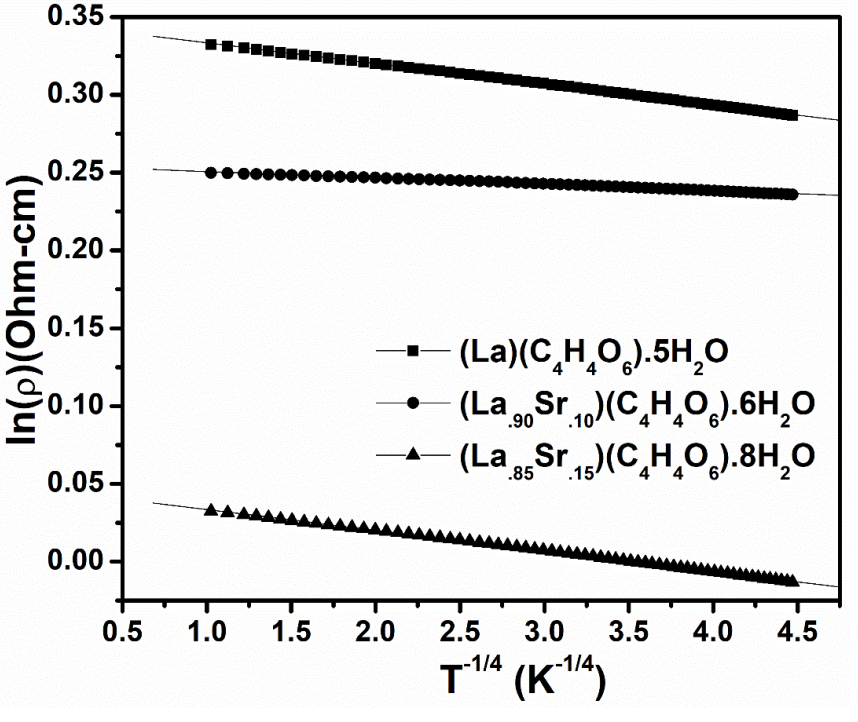

Fig. 3. VRH fit for pure and strontium doped lanthanum tartrate.

The calculated values from equation (7), incorporating K_2, provide load-independent values of Hv:

$$H_v = 1.8544\ k_2 \quad (7)$$

Substituting the respective values of K_2 yields Hv as 73.2 GN/m² for $LaC_4H_4O_6 \cdot 5H_2O$, 108.7 GN/m² for $La_{0.90}Sr_{0.10}C_4H_4O_6 \cdot 6H_2O$, and 128.2 GN/m² for $La_{0.85}Sr_{0.15}C_4H_4O_6 \cdot 8H_2O$.

The experimental data obtained from Figure 4 suggest load-independent values of H_v as 75 GN/m², 110 GN/m², and 130 GN/m² for $(La)C_4H_4O_6 \cdot 5H_2O$, $(La)_{0.90}(Sr)_{0.10}C_4H_4O_6 \cdot 6H_2O$, and $(La)_{0.85}(Sr)_{0.15}C_4H_4O_6 \cdot 8H_2O$, respectively. The experimental values of H_v obtained for all three compositions of spherulites are in close agreement, further supporting the validity of Hays and Kendall's law.

Figure 5 displays the ln(P-W) versus ln d plot used to determine n values, which approximate 2 for all compositions. This suggests that Hv indeed exhibits load-independent behavior in the investigated LaT compositions, reinforcing the validity of Hays and Kendall's law for these polycrystalline materials [27].

Table 2 summarizes the calculated values of nnn using both Kick's and Hays and Kendall's laws. The n_k values, derived from Mayer's law (Kick's law), and n_h, obtained from Hays and Kendall's law, demonstrate consistency across all compositions studied. These findings underscore the robustness of Hays and Kendall's law in describing the mechanical properties of LaT crystals under varying loads.

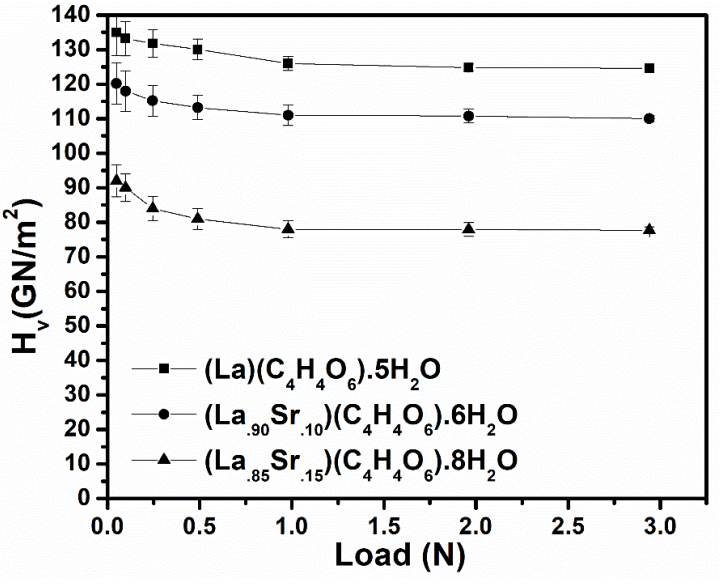

Fig. 4. Graph showing dependence of H_v on load for pure and strontium doped lanthanum tartrate.

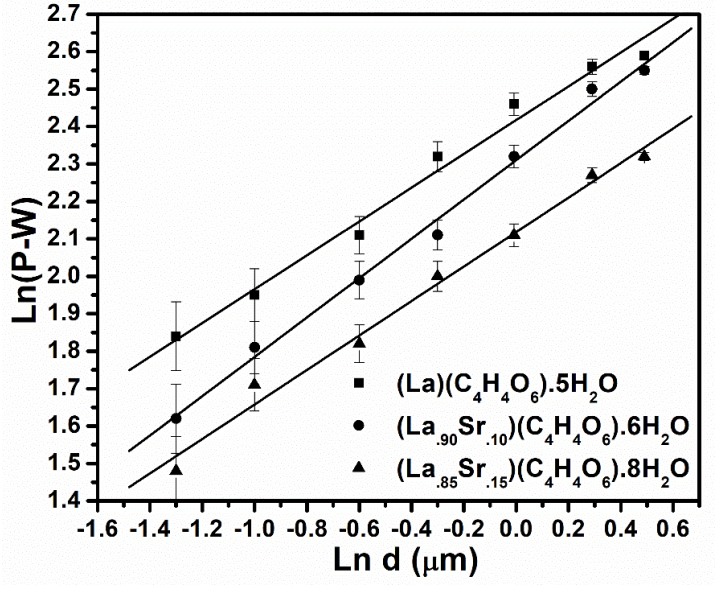

Fig. 5. Graph of ln(P-W) verses Ln d for pure and doped lanthanum tartrate.

Table 2. Value of n calculated using Kick's and Hays and Kendall's law.

Samples	Load range P(N)	H_v (Exp.) GN/m^2	H_v (Cal.) GN/m^2	n_k	n_h
(La) $C_4H_4O_6 .5H_2O$	0.049-2.94	75	73.2	1.63	2.09
(La) $C_4H_4O_6 .5H_2O$	0.049-2.94	110	108.7	1.71	2.11
$(La)_{0.85} (Sr)_{0.15} C_4H_4O_6 .8H_2O$	0.049-2.94	130	128.2	1.74	2.26

n_k value of Mayer's index using Kick's law.

n_h value of Myer's index using Hays and Kendall's law.

The microhardness analysis using Mayer's and Hays and Kendall's laws provides a comprehensive understanding of how strontium doping influences the mechanical properties of lanthanum tartrate spherulites. The observed load-independent values of Hv highlight the material's ability to withstand varying pressures, crucial for applications requiring precise mechanical performance. These insights contribute to the broader understanding and potential optimization of LaT for diverse industrial and technological applications.

4. CONCLUSION

Based on the comprehensive experimental investigations conducted on pure and strontium-doped lanthanum tartrate (LaT) crystals, several significant conclusions can be drawn regarding their electrical and mechanical properties. The electrical resistivity measurements clearly indicate semiconducting behavior in all compositions studied. The resistivity at room temperature decreases as the concentration of strontium increases in lanthanum tartrate. This behavior suggests that the introduction of strontium ions into the LaT lattice alters its electronic structure, enhancing charge carrier mobility and thereby reducing resistivity. The application of Mott's variable-range hopping (VRH) model to fit the resistivity data provides deeper insights into the conduction mechanism. The reduction in the gap parameter from 190.5 to 175.505 meV due to strontium doping indicates that disorder-induced charge carriers play a significant role in the electrical transport properties of these materials. This finding underscores the importance of dopant-induced disorder in facilitating conduction pathways within the crystal lattice. Moving to the mechanical properties, microhardness testing using Hays and Kendall's law reveals consistent and load-independent values of Hv across the applied load range for both pure and strontium-doped LaT crystals. This suggests that the mechanical response of LaT spherulites to indentation follows a predictable pattern, akin to other polycrystalline materials studied under similar conditions. The decrease in saturation Hv values with increasing strontium concentration further corroborates the influence of dopant atoms on the material's mechanical resilience. The experimental findings highlight the multifaceted impact of strontium doping on the physical properties of lanthanum tartrate. The combination of electrical resistivity analysis and microhardness measurements underscores the effectiveness of strontium as a dopant in modifying both electronic and mechanical characteristics. These insights not only contribute to fundamental understanding but also pave the way for potential applications of LaT in semiconductor and mechanical engineering fields where tailored properties are essential. Future research directions may explore additional dopants or optimization strategies to further enhance these desirable properties for practical applications.

CONFLICT OF INTEREST

The authors declare that there is no conflict of interests.

REFERENCES

[1] Torres, M.E., Lopez, T., Peraza, J., Stockel, J., Yanes, A.C., Gonzalez-Silgo, C., Ruiz-Perez, C. and Lorenzo-Luis, P.A., **1998.** Structural and dielectric characterization of cadmium tartrate. *Journal of Applied Physics*, *84*(10), pp.5729-5732.

[2] Torres, M.E., Yanes, A.C., Lopez, T., Stockel, J. and Peraza, J.F., **1995.** Characterization and thermal and electromagnetic behaviour of gadolinium-doped calcium tartrate crystals grown by the solution technique. *Journal of Crystal Growth*, *156*(4), pp.421-425.

[3] Kotru, P.N., Gupta, N.K., Raina, K.K. and Koul, M.L., **1986.** Characterization and thermal behaviour of lanthanum tartrate crystals grown from silica gels. *Bulletin of Materials Science*, *8*, pp.547-555.

[4] Kotru, P.N., Gupta, N.K. and Raina, K.K., **1986.** Growth of lanthanum tartrate crystals in silica gel. *Journal of Materials Science*, *21*, pp.90-96.

[5] Quasim, I., Firdous, A., Want, B., Khosa, S.K. and Kotru, P.N., **2008.** Single crystal growth and characterization of pure and sodium-modified copper tartrate. *Journal of*

Crystal Growth, *310*(24), pp.5357-5363.

[6] Dennis, J. and Henisch, H.K., **1967.** Nucleation and growth of crystals in gels. *Journal of the Electrochemical Society*, *114*(3), p.263.

[7] Rethinam, F.J., Oli, D.A., Ramasamy, S. and Ramasamy, P., **1993.** Growth and Characterisation of Pure and Nickel-doped Strontium Tartrate Tetrahydrate Single Crystals. *Crystal Research and Technology*, *28*(6), pp.861-865.

[8] Satyanarayana, N., Hariharan, K. and Radhakrishna, S., **1985.** Gel growth and characterization of pure and vanadyl-doped strontium tartrate tetrahydrate single crystals. *Journal of Materials Science*, *20*, pp.1993-2000.

[9] Nallamuthu, D., Selvarajan, P. and Freeda, T.H., **2010.** Studies on various properties of pure and Li-doped Barium Hydrogen Phosphate (BHP) single crystals. *Physica B: Condensed Matter*, *405*(24), pp.4908-4913.

[10] Viji, R.K., Gowri, B. and Shajan, X.S., 2005. Some Investigation on Pure and Impurity–Added Strontium Tartrate Trihydrate Crystals. *Indian Journal of Physics*. 12(2), pp. 1373-1376.

[11] Firdous, A., Quasim, I., Ahmad, M.M. and Kotru, P.N., **2009.** Studies on gel-grown pure and strontium-modified lanthanum tartrate crystals. *Journal of Crystal Growth*, *311*(15), pp.3855-3862.

[12] Firdous, A., Quasim, I., Ahmad, M.M. and Kotru, P.N., **2008.** Growth and characterization of strontium tartrate pentahydrate crystals. *Crystal Research and Technology: Journal of Experimental and Industrial Crystallography*, *43*(10), pp.1015-1021.

[13] Arora, S.K., Patel, V., Kothari, A. and Amin, B., **2004**. Gel growth and preliminary characterization of strontium tartrate trihydrate. *Crystal Growth & Design*, *4*(2), pp.343-349.

[14] Firdous, A., Quasim, I., Ahmad, M.M. and Kotru, P.N., **2008.** Growth and characterization of strontium tartrate pentahydrate crystals. *Crystal Research and Technology: Journal of Experimental and Industrial Crystallography*, *43*(10), pp.1015-1021.

[15] Want, B., Ahmad, F. and Kotru, P.N., **2006.** Crystal growth and characterization of gadolinium tartrate trihydrate: Gd $(C_4H_4O_6)(C_4H_5O_6)\cdot 3H_2O$. *Materials Science and Engineering: A*, *431*(1-2), pp.237-247.

[16] Kotru, P.N., Gupta, N.K. and Raina, K.K., **1986.** Growth and kinetic studies of spherulitic gadolinium tartrate crystals from silica gel. *Crystal Research and Technology*, *21*(1), pp.15-22.

[17] Kotru, P.N., Gupta, N.K., Raina, K.K. and Sharma, I.B., **1986.** Characterization and thermal behaviour of gel-grown gadolinium tartrate crystals. *Journal of Materials Science*, *21*, pp.83-89.

[18] Guo, N.J., Li, S., Liu, W., Yang, Y.Z., Zeng, X.D., Yu, S., Meng, Y., Li, Z.P., Wang, Z.A., Xie, L.K. and Ge, R.C., **2023.** Coherent control of an ultrabright single spin in hexagonal boron nitride at room temperature. *Nature Communications*, *14*(1), p.2893.

[19] Tickoo, R., Tandon, R.P., Bamzai, K.K. and Kotru, P.N., **2004.** Indentation induced testing studies on lanthanum modified lead titanate ceramics. *Materials Science and Engineering: B*, *110*(2), pp.177-184.

[20] Lal, B., Bamzai, K.K. and Kotru, P.N., **2003.** Mechanical characteristics of melt grown doped $KMgF_3$ crystals. *Materials chemistry and physics*, *78*(1), pp.202-207.

[21] Joseph, A.J., Sinha, N., Goel, S., Hussain, A. and Kumar, B., **2020.** True-remanent, resistive-leakage and mechanical studies of flux grown 0.64 PMN-0.36 PT single crystals. *Arabian Journal of Chemistry*, *13*(1), pp.2596-2610.

[22] Gupta, V., Bamzai, K.K., Kotru, P.N. and Wanklyn, B.M., **2005.** Mechanical characteristics of flux-grown calcium titanate and nickel titanate crystals. *Materials chemistry and physics*, *89*(1), pp.64-71.

[23] Jung, Y.S., Jung, W. and Ross, C.A., **2008.** Nanofabricated concentric ring structures by templated self-assembly of a diblock copolymer. *Nano Letters*, *8*(9), pp.2975-2981.

[24] Mott, N.F., **1980.** States in the gap in non-crystalline semiconductors. *Journal of Physics C: Solid State Physics*, *13*(30), p.5433.

[25] Maignan, A., Hébert, S., Pi, L., Pelloquin, D., Martin, C., Michel, C., Hervieu, M. and Raveau, B., **2002.** Perovskite manganites and layered cobaltites: potential materials for thermoelectric applications. *Crystal Engineering*, *5*(3-4), pp.365-382.

[26] Turkoz, M.B., Nezir, S., Ozturk, O., Asikuzun, E., Yildirim, G., Terzioglu, C. and Varilci, A., **2013.** Experimental and theoretical approaches on mechanical evaluation of Y123 system by Lu addition. *Journal of Materials Science: Materials in Electronics*, *24*, pp.2414-2421.

[27] Jethva, H.O., Dabhi, R.M. and Joshi, M.J., **2016.** Structural, spectroscopic, magnetic and thermal studies of gel-grown copper levo-tartrate and copper dextro-tartrate crystals. *IOSR Journal of Applied Physics*, *8*(3), pp.33-42.

